Brain-penetrant dual ATR-mTOR inhibitors for PTEN-deficient cancers

Sarah Truong[1,2,3], Louise Ramos[1,2,3], Fariba Ghaidi[1,2,3], Mona Marzban[1,2,3], Brian Atwood[4], Marshall Drew-Brook[4], Pete Guzzo[4], Ahmad Issa[4], Mehran Khodabandeh[4], Sara Omar[4], Jason Rolfe[4], Seyed Ali Saberali[4], Maxence Bos[5], Julien Breault-Turcot[5], Yuniel Fernandez[5], Felicia Lim[5], Yael Mamane[5], Leonie Norris[5], Niaz Oliazadeh[5], Yassine Oufqir[5], Mehrnaz Pourashra[5], Daniel Therien[5], Vouy Linh Truong[5], Kally Singh[2], John Langlands[2], Dennis Brown[2], Jeffrey Bacha[2], & Mads Daugaard[1,2,3,6]

[1]Vancouver Prostate Centre, Vancouver, BC, Canada; [2]Rakovina Therapeutics, Vancouver, BC, Canada; [3]M. H. Mohseni Institute of Urologic Sciences, Vancouver, BC, Canada; [4]Variational AI, Vancouver, BC, Canada, [5]Sygnature Discovery, Nottingham, United Kingdom; [6]Department of Urologic Sciences, University of British Columbia, Vancouver, BC, Canada

Introduction

Ataxia telangiectasia and Rad3-related (ATR) kinase is a master regulator of the DNA damage response and helps maintain genomic stability. Cancer cells often upregulate ATR to survive replication stress. Inhibiting ATR stalls replication forks, arrests the cell cycle, and causes accumulation of DNA damage[1].

Many tumor types are sensitive to ATR inhibitors (ATRi), but these agents are usually tested clinically in combination with other therapies or in tumors carrying genetic vulnerabilities that increase sensitivity[2]. PTEN loss is one such vulnerability: ATRi are synthetically lethal in PTEN-deficient cells[3–5]. PTEN restrains PI3K–Akt signaling and contributes to cell cycle control and DNA repair, in part through Chk1 — the same checkpoint effector activated by ATR[6]. Cells lacking PTEN, therefore, depend on ATR–Chk1 signaling to manage replication stress, and inhibiting ATR removes that remaining safeguard, leading to genomic instability, DNA damage and cell death.

PTEN deficiency occurs in up to 40% of gliomas[7] and 63% of breast cancers[8], a cancer that frequently metastasizes to the brain. Because PTEN loss also hyperactivates PI3K–mTOR signaling, this program initially targeted dual ATR/mTOR inhibition. After evaluation of several compound families, we maintained selective potency against ATR with variable potency against mTOR. Lead optimization converged instead on ATR-selective compounds, avoiding confounding toxicity associated with added mTOR blockade while retaining activity in PTEN-deficient glioblastoma cells. Here we describe brain-penetrant, ATR-selective inhibitors developed for PTEN-deficient CNS tumors.

Table 1. Summary of percentage of cancer patients with PTEN deficiency in various cancer indications

Indication	Patients with PTEN deficiency (%)	References
Glioma	5–40	Koschmann et al. (2017) NPJ Precis Oncol. Han et al. (2016) Onco Targets Ther.
Breast cancer	4–63	Li et al. (2017) Oncotarget
Lung cancer	15–38	Fischer et al. (2022) Cell BioSci.
Melanoma	5–59	Wu et al. (2003) Oncogene Cabrita et al. (2020) Cancers

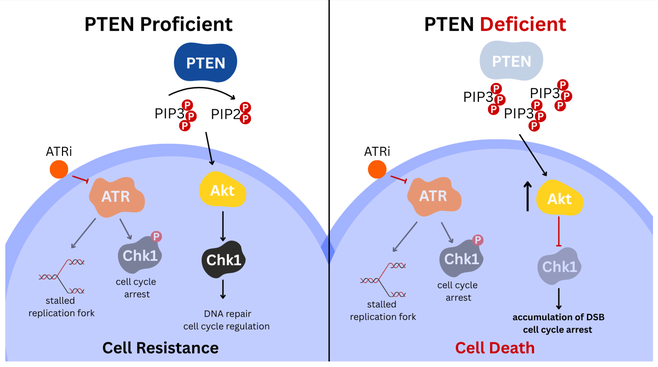

Figure 1. Proposed mechanism of PTEN synthetic lethality with ATR inhibition

Molecules were designed *de novo* using Enki™, a generative AI platform that applies a latent diffusion model to optimize many properties simultaneously — potency against the primary target, selectivity, ADMET and physicochemical properties — against a target product profile requiring CNS penetration. The most promising molecules were synthesized and tested. We present *in vitro* potency and selectivity, cell viability and ADME data for five lead compounds.

CNS Penetration

	Molecular Weight	cLogP	TPSA	Hydrogen Bond Donors	BBB Score
Compound A	385.5	2.72	76.3	1	0.68
Compound B	385.5	2.72	76.3	1	0.75
Compound C	397.5	2.86	76.3	1	0.86
Compound D	366.4	2.66	79.9	0	0.91
Compound E	368.5	2.90	79.9	0	0.93

Compounds were designed and filtered on physicochemical criteria associated with CNS penetrance and reduced efflux liability: molecular weight <450 kDa, cLogP 2-4, tPSA < 90, and hydrogen bond donors ≤2. BBB score is a probability of being able to cross the blood brain barrier, where a value of 1 is predicted to cross and 0 is predicted to not be able to cross the blood brain barrier.

References

1. *Fokas E, Prevo R, Hammond EM, Brunner TB, McKenna WG, Muschel RJ. Cancer Treat Rev. 2014 Feb;40(1):109-17. doi: 10.1016/j.ctrv.2013.03.002.*
2. *Yano K, Shiotani B.. Cancer Sci. 2023 Jul;114(7):2709-2721. doi: 10.1111/cas.15845.*
3. *Al-Subhi N, Ali R, Abdel-Fatah T, Moseley PM, Chan SYT, Green AR, Ellis IO, Rakha EA, Madhusudan S. Breast Cancer Res Treat. 2018 Jun;169(2):277-286. doi: 10.1007/s10549-018-4683-4*
4. *Hao J, Kochupurakkal B, Branigan TB, Somuncu OS, Liu R, Jadhav H, da Costa AABA, Jiao Y, Martignetti DB, Sadatrezaei G, Mukkavalli S, Gokhale PC, Giumtoli RL II, Martin L, Tanyi J, Latif N, Heller I, Simpkins F, Parmar K, D'Andrea A, Shapiro GI. Mol Cancer Ther 2025 Oct; 24 (10_Supplement): A032. doi.org/10.1158/1535-7163.TARG-25-A032*
5. *Jamaspishvili T, Berman DM, Ross AE, Scher HI, De Marzo AM, Squire JA, Lotan TL. Nat Rev Urol. 2018 Apr;15(4):222-234. doi: 10.1038/nrurol.2018.9.*
6. *Ertay A, Ewing RM, Wang Y. Genes Dis. 2023 Nov;10(6):2511-2527. doi: 10.1016/j.gendis.2022.12.015.*
7. *Li S, Shen Y, Wang M, Yang J, Lv M, Li P, Chen Z, Yang J. Oncotarget. 2017 May 9;8(19):32043-32054. doi: 10.18632/oncotarget.16761.*
8. *Lorente-Macías Á, Mok J, Dawson JC, Juan-Albuquerque A, Carragher NO, Frame MC, Unciti-Broceta A. J Med Chem. 2026 Apr 12. doi: 10.1021/acs.jmedchem.6c00541.*

Inhibition of ATR Enzymatic Activity

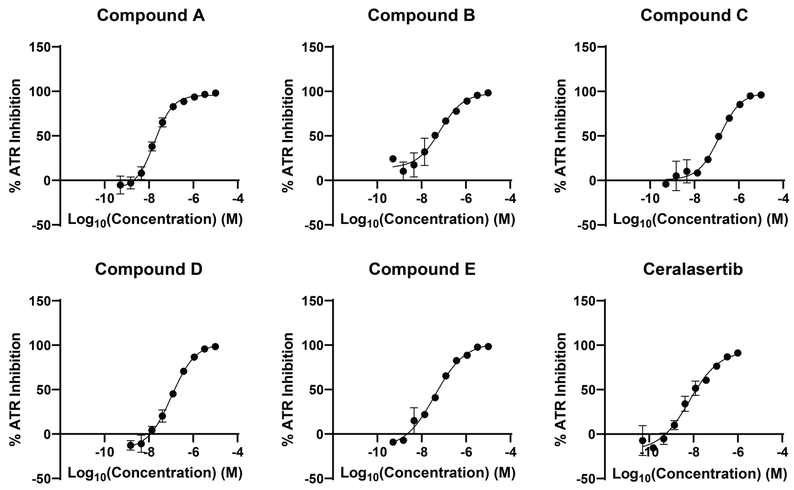

Figure 2. Dose–response inhibition of recombinant ATR [ATR/ATRIP] kinase activity. K_i values derived from IC_{50} using the Cheng–Prusoff equation at K_{mATP} = 12 nM. Representative data of one experiment, mean ± SD of technical duplicates.

Table 2:		
	ATR K_i (nM)	Compared with ceralasertib
Compound A	0.09	2.9× more potent
Compound B	0.16	1.6× more potent
Compound C	0.54	2.1× less potent
Compound D	0.42	1.6× less potent
Compound E	0.16	1.6× more potent
Ceralasertib	0.26	

66 Enki™-designed compounds were screened against recombinant ATR. The five lead compounds shown are potent, sub-nanomolar ATR inhibitors (Ki 0.09–0.54 nM), comparable to the clinical benchmark ceralasertib (Ki 0.26 nM). Compound A was the most potent (~3-fold more potent than ceralasertib), and all compounds fell within ~3-fold of the reference. High intrinsic potency is critical for CNS indications, where unbound brain exposure is typically lower than in plasma.

Selectivity vs. PIKK Kinases

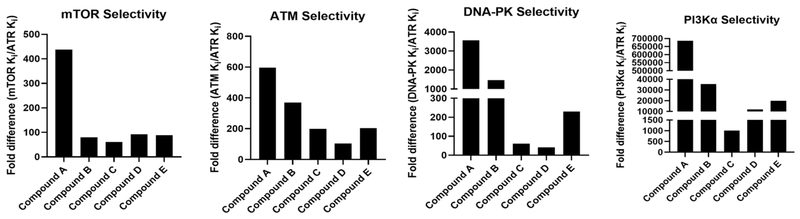

Figure 3. Fold difference of K_is for ATR over mTOR, ATM, DNA-PK, and PI3Kα. K_i values derived from IC_{50} using the Cheng-Prusoff equation using K_{mATP} = 12 nM, 227 nM, 226 nM, 30 µM and 317 µM respectively. Representative data of one experiment, mean ± SD of technical duplicates.

All five compounds are highly selective for ATR over the related PIKK family kinases mTOR, ATM and DNA-PK (≥40-fold), and over the lipid kinase PI3Kα (up to ~680,000-fold). Compound A showed the broadest selectivity (>400-fold against all 4 kinases).

Selective ATR inhibition limits the toxicities associated with blocking related kinases: ATM and DNA-PK inhibition sensitizes normal tissue to DNA damage, and PI3K/mTOR inhibition carries metabolic liabilities. A clean profile supports future combination with radiotherapy and temozolomide, standard of care in glioma.

In vitro Metabolic Stability

Table 3	Mouse liver microsomes		Human liver microsomes	
	$T_{1/2}$ (min)	Cl_{int} (µL/min/mg)	$T_{1/2}$ (min)	Cl_{int} (µL/min/mg)
Compound A	72.6	19.9	336.5	4.1
Compound B	47.1	29.5	63.8	21.8
Compound C	52.7	27.6	103.7	13.6
Compound D	52.5	27.0	67.9	20.6
Compound E	69.5	21.1	365.2	3.8

In liver microsome stability assays, all five compounds showed low to moderate intrinsic clearance in mouse (Clint 19.9–29.5 µL/min/mg; $T_{1/2}$ 47–73 min) and lower clearance in human (Clint 3.8–21.8 µL/min/mg; $T_{1/2}$ 64–365 min). Compounds A and E were the most stable, with human $T_{1/2}$ exceeding 5 hours and Clint below 5 µL/min/mg.

Low hepatic clearance supports sustained oral exposure and a practical dosing regimen.

MDCK-MDR1 Permeability

Table 4:	P_{app} ×10^{-6} (cm/s)		Efflux ratio
	A to B	B to A	
Compound A	8.3	17.5	2.11
Compound A + MDR1 inhibitor	10.7	15.5	1.45
Compound B	9.4	12.7	1.36
Compound B + MDR1 inhibitor	17.2	12.1	0.70

Compounds A and B showed high apparent permeability across MDCK-MDR1 monolayers (Papp A→B 8.3 and 9.4 ×10^{-6} cm/s). Efflux ratios were low (2.11 and 1.36) and were further reduced in the presence of an MDR1 inhibitor (1.45 and 0.70), indicating only minimal P-glycoprotein-mediated efflux.

These data support the design objective of these brain-penetrant ATR inhibitors; in vivo brain-to-plasma exposure studies are ongoing.

CNS Tumor Cell Viability

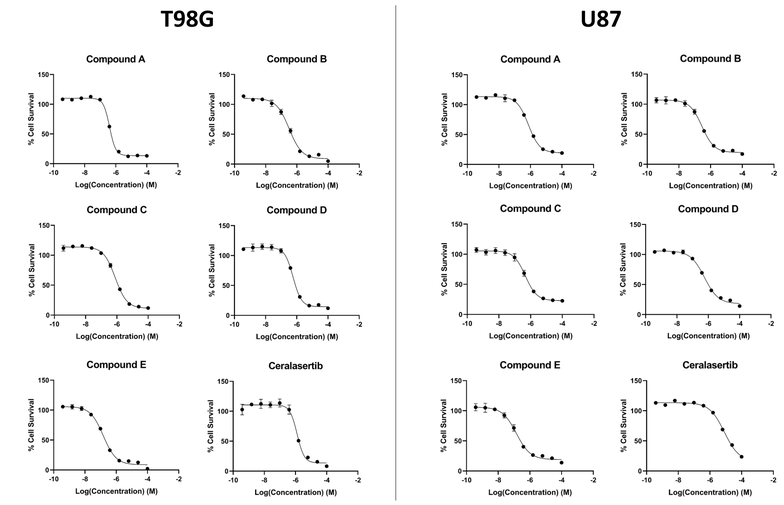

Figure 4: Viability of glioblastoma cell lines T98G and U87 after treatment of cells for 72 h; viability by GlowQuant™ cell viability assay. EC_{50} from four-parameter fits, representative data of one experiment, mean ± SD of technical triplicates..

Table 5:	A	B	C	D	E	Ceralasertib
T98G EC_{50} (µM)	0.19	0.28	0.78	0.57	0.14	1.3
U87 EC_{50} (µM)	0.31	0.20	0.46	0.56	0.14	8.1

All five compounds inhibited viability of the PTEN-mutant glioblastoma lines T98G (left) and U87 (right) after 72 hours, with EC_{50} values of 0.14–0.78 µM. All compounds were more potent than ceralasertib in both lines — up to 9-fold in T98G and 58-fold in U87 — with compound E the most potent (0.14 µM in both).

Potency was consistent across the two lines, whereas ceralasertib was six-fold weaker in U87 than T98G. Sub-micromolar activity in glioblastoma cells, combined with the ATR selectivity and metabolic stability shown here, supports further evaluation of these compounds in PTEN-deficient CNS tumours.

Conclusions and Future Directions

- Using the Enki™ generative AI platform, we designed and synthesized novel ATR inhibitors against a target product profile combining potency, selectivity and CNS penetration.
- From 89 in silico designs, 66 compounds were synthesized and evaluated over a 6-month period
- Lead compounds are sub-nanomolar ATR inhibitors (K_i 0.09–0.54 nM) with ≥40-fold selectivity over ATM, DNA-PK and mTOR, and over PI3Kα.
- All compounds were more potent than ceralasertib against PTEN-mutant glioblastoma lines — up to 9-fold in T98G and 58-fold in U87.
- Compounds showed low intrinsic clearance in human liver microsomes, together with high permeability and minimal P-gp efflux in MDCK-MDR1 — an in vitro profile consistent with CNS exposure.
- Ongoing work includes *in vivo* brain-to-plasma exposure, intracranial xenograft efficacy, and comparison of PTEN-deficient versus PTEN-proficient models.

RAKOVINA THERAPEUTICS INC. · VARIATIONAL AI · M.H. Mohseni Institute of Urologic Sciences

THE UNIVERSITY OF BRITISH COLUMBIA · VANCOUVER PROSTATE CENTRE, A UBC & VGH Centre of Excellence